



Research article

Vascular endothelial and smooth muscle cell galvanotactic response and differential migratory behavior

Kaitlyn R. Ammann^a, Marvin J. Slepian^{a,b,c,*}^a Department of Medicine, Sarver Heart Center, College of Medicine, University of Arizona, Tucson, AZ, 85721, USA^b Department of Biomedical Engineering, University of Arizona, Tucson, AZ, 85721, USA^c Department of Materials Science and Engineering, University of Arizona, Tucson, AZ, 85721, USA

ARTICLE INFO

ABSTRACT

Keywords:
 Galvanotaxis
 Electrotaxis
 Cell migration
 Vascular cell
 Endothelial cell
 Smooth muscle cell
 Cell growth
 Wound healing

Chronic disease or injury of the vasculature impairs the functionality of vascular wall cells particularly in their ability to migrate and repair vascular surfaces. Under pathologic conditions, vascular endothelial cells (ECs) lose their non-thrombogenic properties and decrease their motility. Alternatively, vascular smooth muscle cells (SMCs) may increase motility and proliferation, leading to blood vessel luminal invasion. Current therapies to prevent subsequent blood vessel occlusion commonly mechanically injure vascular cells leading to endothelial denudation and smooth muscle cell luminal migration. Due to this dichotomous migratory behavior, a need exists for modulating vascular cell growth and migration in a more targeted manner. Here, we examine the efficacy of utilizing small direct current electric fields to influence vascular cell-specific migration ("galvanotaxis"). We designed, fabricated, and implemented an *in vitro* chamber for tracking vascular cell migration direction, distance, and displacement under galvanotactic influence of varying magnitude. Our results indicate that vascular ECs and SMCs have differing responses to galvanotaxis; ECs exhibit a positive correlation of anodal migration while SMCs exhibit minimal change in directional migration in relation to the electric field direction. SMCs exhibit less motility response (i.e. distance traveled in 4 h) compared to ECs, but SMCs show a significantly higher motility at low electric potentials (80 mV/cm). With further investigation and translation, galvanotaxis may be an effective solution for modulation of vascular cell-specific migration, leading to enhanced endothelialization, with coordinate reduced smooth muscle in-migration.

Credit author statement

Kaitlyn R Ammann, PhD conceptualized and developed methodology, validated methods, curated and analyzed data, and wrote and revised the manuscript. Marvin J Slepian, MD conceptualized project, reviewed and edited manuscript, and supervised the study.

1. Introduction

Cell growth and migration are crucial in many physiological and pathological processes [1,2]. In the vasculature in particular, integrity of constituent vessel wall cells, i.e. smooth muscle cells (SMCs) and endothelial cells (ECs), are essential for maintenance of local wall function and in assuring uninterrupted blood flow and nutrient transport. As such, maintenance of healthy vascular wall cell phenotype and behavior are central to the balance between normal homeostasis and the

development and progression of disease [3,4]. Atherosclerosis, a common form of vascular disease involving large and medium sized arteries is associated with local vessel wall SMC attenuation with media thinning, and endothelial dysfunction with matrix deposition and intimal thickening [5,6]. This pathology is frequently associated with EC denudation, vulnerable plaque rupture and thrombotic occlusion [7,8], clinically manifesting as myocardial infarction, stroke, or lower limb claudication and ischemia.

A primary therapy for stenotic or occlusive atherosclerosis is percutaneous catheter intervention (PCI). In PCI, the local vascular stenosis or thrombotic occlusion is mechanically dilated via angioplasty balloon catheter and frequently further stabilized with placement of a drug-eluting stent [9–11]. While effective to mechanically re-configure the arterial lumen, PCI with drug-eluting stent(DES), remains hampered by delayed and limited re-endothelialization of DES treated surfaces due to cytotoxic drug elution, necessitating prolonged dual

* Corresponding author. Department of Medicine, Sarver Heart Center, College of Medicine, University of Arizona, Tucson, AZ, 85721, USA.

E-mail addresses: krammann@email.arizona.edu (K.R. Ammann), slepian@email.arizona.edu (M.J. Slepian).

antiplatelet therapy for patients [12,13]. Without healthy, non-thrombogenic endothelial regrowth, the stent and underlying denuded arterial surface remain vulnerable to thrombosis years following DES deployment [14,15]. As such, a need exists for effective local vessel wall passivation and re-endothelialization, i.e. to develop non-drug methods that will reduce SMC luminal invasion post-PCI injury, while coordinately enhancing re-endothelialization of the blood vessel intima.

Similar to other adherent cell types, vascular cells respond to signaling gradients, cueing directional growth and migration. In vascular injury and disease, exposure of medial SMC layers to blood and growth factors, creates a biochemical concentration gradient that cues vascular SMCs to migrate towards the lumen [16]. While this is an example of chemotaxis, there are many other forms of gradient cues or “taxes” which can emit directional cues for cells to migrate. In recent years, physical or mechanical gradients have been explored including durotaxis (substrate stiffness gradient), haptotaxis (substrate adhesion gradient), and to a limited extent galvanotaxis (electric field gradient) [17–20]. While the impact of durotaxis and haptotaxis on vascular cell motility has been explored, the response of vascular cells to electric stimulation gradients, i.e. galvanotaxis, is poorly understood. Current galvanotaxis research on vascular cell growth focuses on enhancing or inhibiting ECs alone for angiogenesis applications, while exploration of galvanotactic effects on vascular SMCs and differential wound healing has been minimal [21–24]. Furthermore, receptivity of cells to these gradients are often cell-type and tissue-source dependent [20,25–28]. For example, bovine corneal epithelial cells, human keratinocytes, amphibian neural crest cells, and mouse embryo fibroblasts have all been demonstrated to migrate towards the cathode [29–31]; whereas human granulocytes, rabbit corneal endothelial cells, and metastatic human breast cancer cells migrated towards the anode [32,33]. Notably, one suggested mechanism of galvanotactic cell behavior is based on ion re-distribution in the cell in response to the applied electric field—

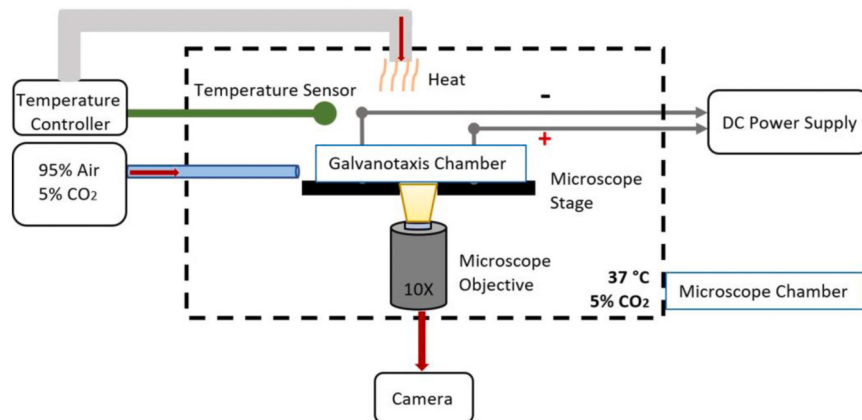
particularly calcium—which can lead to polarization of the cell via calcium-dependent pathways and ultimately impact actin dynamics required for migration [34,35]. Because cells have a varying degree of ion channels and calcium storage to perform their physiologic function, it is therefore possible that their migration response to electric field may differ as well. As such, here we aimed to examine and directly compare the galvanotactic migratory response of primary vascular ECs and SMCs derived from human umbilical blood vessels. We hypothesized that small direct current electric fields (DCEFs) will have defined, differing effect on ECs and SMCs that will lead to differential changes in their motility or directional growth. To address this hypothesis, we first developed and validated a novel single-chip galvanotaxis chamber, allowing for live-cell imaging and analysis. We then examined and quantified EC and SMC migration, direction, and extent as they relate to DCEF magnitude and direction.

2. Results

2.1. Galvanotaxis platform design and validation

Cell viability was maintained during galvanotaxis experiments through utilization of a controlled-environment microscope chamber (Fig. 1). Temperature, CO₂ levels, and relative humidity were all regulated within the microscope chamber, allowing for live-cell imaging of migrating cells (Fig. 1A). The galvanotaxis platform, consisting of multiple reservoirs, additionally allowed for DCEFs to be applied across the cell chamber without the introduction of electrolysis to the media (Fig. 1B). Specifically, the direct current (DC) was applied to a conductive solution (Ag/AgCl electrodes in saline) and the electric potential generated in the saline wells created an ion polarization that could be transferred through the agar salt bridges on either end of the cell chamber, creating an electrolytic-free, ion-driven electric potential (Fig. 1B).

A Environmental Microscope Chamber Set-Up



B Galvanotaxis Chamber Set-Up

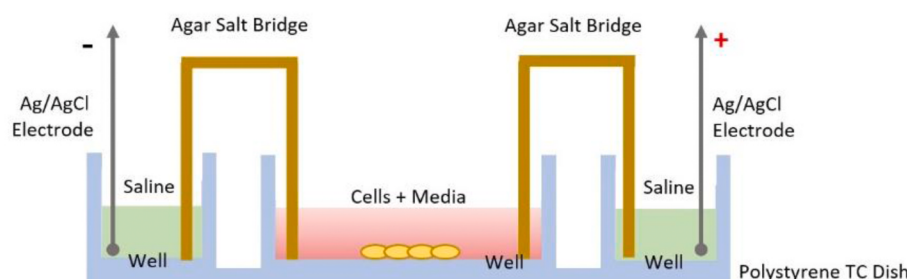


Fig. 1. Galvanotaxis System Overview.
(A) Galvanotaxis of vascular cells was observed using an environmental chamber around a Zeiss Axiovert 135 microscope. The chamber was maintained at 37 °C and 5% CO₂ for the duration of the experiment using a temperature sensor/controller feedback system and an external compressed gas tank (95% Air/5% CO₂). The cells inside the galvanotaxis chamber were visualized through the microscope objective (10×) that was connected to an external camera, taking images of the cells every 5 min. **(B)** The galvanotaxis chamber was designed to fit the microscope stage, allowing cells to be visualized in the center chamber during DCEF application. Voltage from an external DC power supply was applied directly to two chambers of saline buffer with Ag/AgCl wires; DCEFs were mediated across the cells with 2% (w/v) agar bridges on either side of the cell chambers.

Traditionally, galvanotaxis experiments utilize multiple dishes or plates, physically separating the saline wells from the cell chamber. To enhance reproducibility and improve ease-of-use, we created a 3-D printed platform with multiple wells to incorporate all elements needed in the galvanotaxis set-up (Fig. 2A). The platform was designed to fit in a 60 mm polystyrene dish that could easily be secured to a microscope stage. The chamber additionally incorporated holes for securing electrodes and bridges consistently, providing reproducible and uniform electric field (EF) application. Fig. 2B displays top and side views of the final 3-D printed platform with connected agar salt bridges and electrodes within the 60-mm dish.

To validate uniform DCEF across the cell chamber, Fig. 3A depicts the results of simulating a 10 V electric potential across the cell chamber from secured agar bridges. Although 10 V is higher than any electric potential that would be used in translation of this approach, the EFs were still uniform across the cell imaging area. The DCEF application was further verified by measuring electric potential on either side of the cell chamber in both EC growth medium and SMC growth medium. Results indicated the relationship between applied and measured voltage was linear ($R^2 > 0.9$; Fig. 3B). EC medium showed a less positive correlation between measured voltage and applied voltage, indicating lower conductivity (approximately 14 mS) than EC growth medium (approximately 12 mS). As such, applied voltages did not correspond to equal measured voltages between the ECs and SMCs.

After exposure to DCEFs, captured video from a microscope camera allowed tracking of cell migration paths. Cell migration paths were identified as an x-y position in relation to their starting point. In order to directly compare cell tracks, the cell positions and resultant paths were translated to begin at the x-y origin (0,0) of the cell track plots (Fig. 4A). From these positions, their directional alignment to the applied DCEF, distance and displacement traveled from their starting point were quantified as depicted in Fig. 4B.

From quantified EC migration paths, results indicated that EC motility increased with increasing voltage magnitude applied. Specifically, with 200 V application, the EC distance was significantly greater

than distances traveled between 0 and 60 V application (Fig. 5A). However, the displacement of ECs at 200 V was lower, suggesting the EC migration path was not in a consistent direction (Fig. 5B). In contrast, application of 100 V also led to increased distance traveled by ECs, but also displacement compared to lower voltages applied (e.g. 40 and 50 V). Although not significant, the motility was interestingly lower between 40 V and 60 V of applied voltage in comparison to no DCEF (0 V) control. In contrast, SMC motility was markedly unchanged by application of voltage, regardless of voltage magnitude (Fig. 5C and D). While there were some increases seen in overall average distance traveled by SMCs in comparison to 0 V control, none of these differences were statistically significant.

When examining the migration direction of ECs and SMCs in relation to the DCEF direction, we found significant changes with EC migration direction with increasing voltage magnitude. ECs migrated towards the cathode at lower applied voltages, with low voltage (40 V) application exhibiting significantly more directionality than without voltage ($p < 0.05$). However, average EC migration direction changed at 100 V and began migrating towards the anode at 100 V and 200 V application, with significant ($p < 0.01$) difference in directionality compared to the lower voltage applications (Fig. 6A). SMCs, however, were less responsive to the EF magnitude changes and exhibited more random directionality with average directionality centered around $\cos(\Theta) = 0$, or perpendicular to the field. Between the 40 V and 200 V applied, there was a slight trend of SMCs migrating towards the electrical cathode with increasing voltage, however this change was not significant (Fig. 6B).

Because the EC and SMC media had different conductivities, the electric potential experienced by the cells with the same applied voltage was different. To directly compare the two cell types in their respective media, we examined migration characteristics of both ECs and SMCs when the measured electric potential directly across the cell chamber were similar (± 5 mV/cm). First examining migration directionality, we see the biggest differences between EC and SMC migration direction occur at lower electric potentials (80 mV/cm; $p < 0.005$) (Fig. 7A). However, SMC distance (Fig. 7B) and displacement (Fig. 7C) were

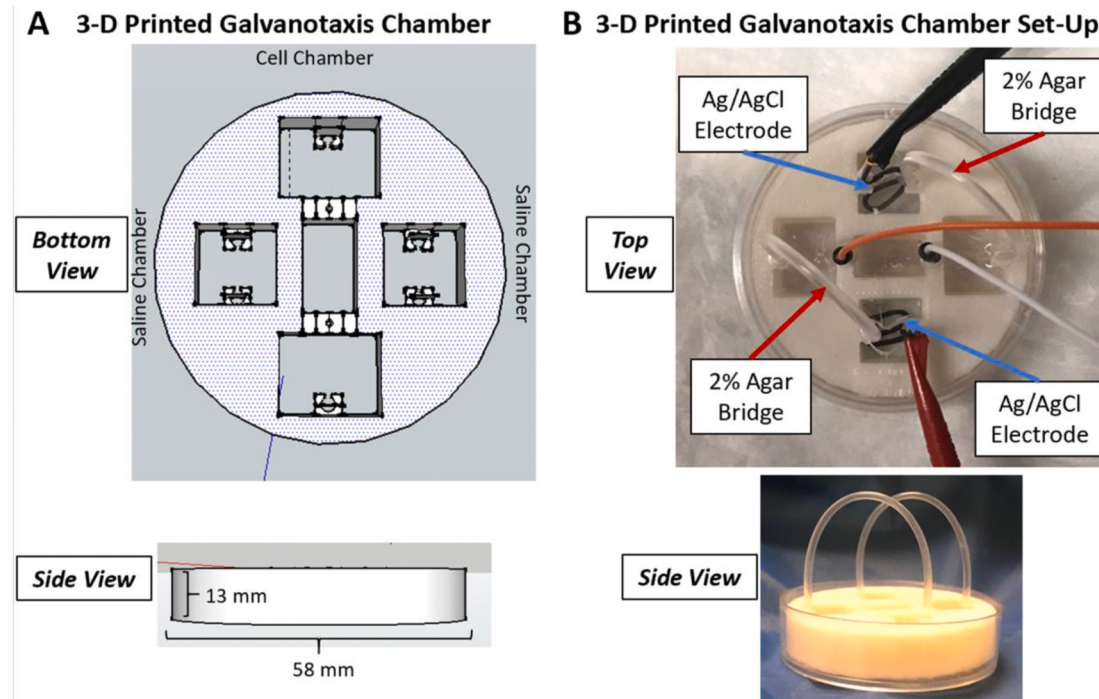
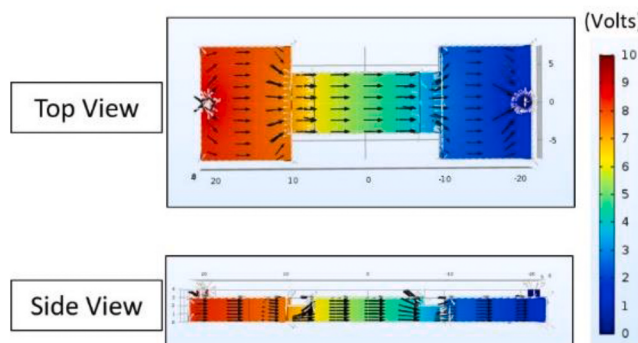


Fig. 2. Single Unit Galvanotaxis Chamber Design and Set-Up. (A) The galvanotaxis chamber was designed and 3-D printed to incorporate multiple wells into a single unit that fits within a 60-mm polystyrene dish. The design incorporates two saline buffer chambers and a single, elongated cell chamber for seeding and visualization of cells. Holes were added to the sides of each well for securing electrodes and agar bridges. (B) After the chamber is 3-D printed and secured to the polystyrene dish (with silicone grease), electrodes, salt bridges can be added for experimentation.

A Electric Field Model in Cell Chamber



B Electric Field Measurement in Cell Chamber

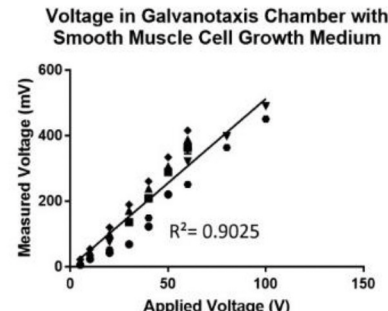
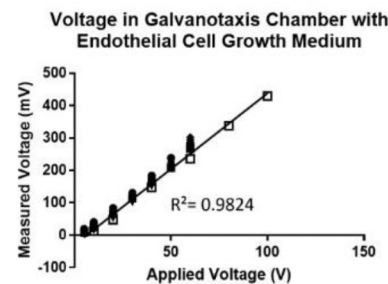


Fig. 3. Galvanotaxis Chamber Validation. (A) Application of 10 V across cell chamber through agar bridges was simulated in COMSOL to ensure uniform DCEF across cells. (B) A range of voltages were applied to the galvanotaxis chamber and then measured across the cell chamber for both EC growth medium (top) and SMC growth medium (bottom). Measured versus applied voltages had significantly linear relationships for both cell media ($N = 5$).

greater than that of ECs at lower electric potentials. These results suggest that 80 mV/cm electric potential has the most significant differential effect on EC versus SMC migration directionality, distance, and displacement, with ECs migrating towards the cathode and SMCs lacking significant directionality. SMCs, however, migrate significantly farther than ECs at 80 mV/cm. In contrast, 130 mV/cm electric potential caused statistically similar migratory behavior between ECs and SMCs.

3. Discussion

The objective of this study was to examine the response of endothelial and smooth muscle cells to galvanotactic stimuli and determine the ability of galvanotaxis to differentially modulate migration of vascular ECs versus SMCs. Our results indicate that ECs and SMCs indeed have a differential response to DCEFs, with ECs migrating towards the anode with increasing voltage magnitude, while SMCs remain statistically unresponsive over the range of voltage tested. Similarly, the motility, i.e. the distance and displacement traveled, of ECs increased while SMCs stayed the same. However, when directly comparing ECs to SMCs by electric potential, the optimal EF was not clearly defined. Of the ranges explored here (0–130 mV/cm), 80 mV/cm is optimal in terms of directionality between SMCs versus ECs; however, SMCs migrate further than ECs at this electric potential. While this is not ideal for reducing SMC migration into the lumen of an artery, the increased directionality and motility of ECs is still valuable for enhancing re-establishment of an endothelial barrier between the blood and vascular medial layer, subsequently reducing chronic inflammation, SMC activation, and SMC migration towards the lumen.

3.1. Electric field considerations in galvanotaxis

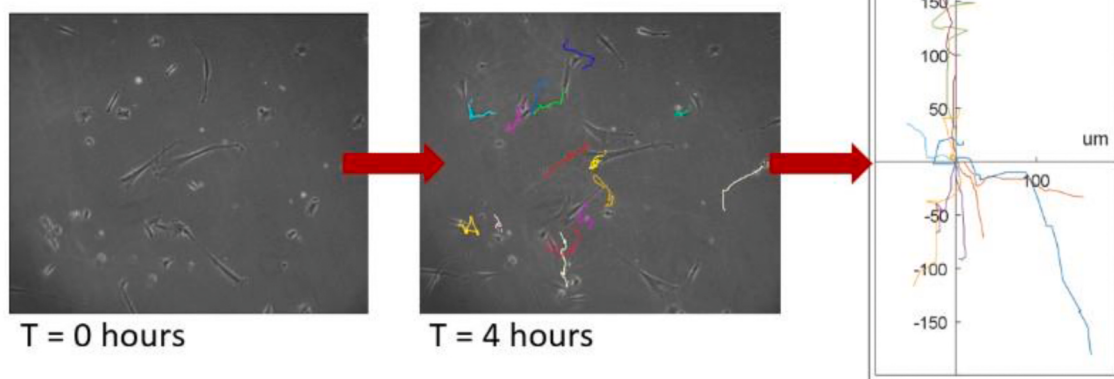
While numerous platforms have been developed in the past decade for studying galvanotaxis *in vitro*, our design allowed for the electrolytic saline chambers and cell chambers to be incorporated into a single cohesive unit [26,28,36]. The platform described here, facilitated

reproducibility and simple comparison between behavior of the two cell types. Additionally, the modularity of the platform afforded the ability to optimize agar bridge dimensions and compositions, as well as explore various electrolytes and media concentrations. Prior studies have reported current density ($\mu\text{A}/\text{cm}^2$) as opposed to electric potential (V/cm) as a driving factor in galvanotactic behavior [37,38]. While the measured current for our experiments and electric potential ranges remained low (μA to mA range) the platform cross-sectional area could easily be adjusted for future examination of current density. Furthermore, translation to use in actual 3-D tissue environments would likely require higher voltages for transmittance through dense connective tissues, which could easily be simulated in the described galvanotaxis platform. Some galvanotactic studies have modulated cell growth with alternating current (AC) [39,40]; however, in this study, DC application was required due to the use of electrolytic chambers (i.e. electrodes were not applied directly to cell media) to prevent media electrolysis. Cell death from electrolysis can occur when free electrons from the electrical current react with the ions in the media, producing toxic compounds [41,42]. Electrolytic chambers allow for electrolysis to occur in isolated reservoirs in which the salt bridge is used to balance the reaction, driving an ionic instead of electron current across the cells. With AC, the electrochemical reaction would be unable to establish polarity across the cell chamber since the positive and negative charge in the electrolytic saline chambers would constantly be oscillating. Therefore, AC would need to be applied directly to the media, which would only be viable with heavier, chemically inert metals and lower, non-toxic voltage magnitudes. Because our results indicate low-magnitude DCEFs as optimal, direct electrode application utilizing AC could be possible for future studies.

3.2. Biological considerations in galvanotaxis

While galvanotactic signaling in cells is not yet fully understood, the leading theory suggests that wounding generates an ion-driven electric potential difference between the apical and basal surface of a wound,

A Tracking Cell Migration



B Cell Path Quantification and Electric Field Relationship

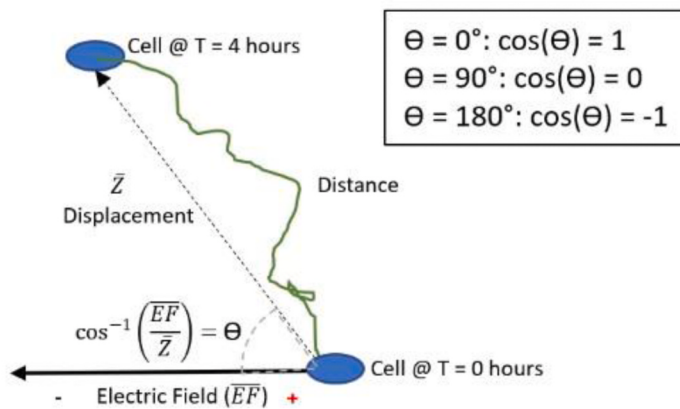


Fig. 4. Galvanotaxis Procedure and Analysis. (A) Cells in galvanotaxis chamber are imaged over 4 h at 5-min intervals. Resultant stacked images create a video in which individual cell paths are tracked in 2-D (x,y) and quantified in μm . All cell paths are normalized to start at (0,0) origin before quantification. Displayed graph represents data from 100V applied to SMCs over 4 h. (B) Each cell path's distance and displacement are quantified in μm from the origin. The displacement and DCEF are denoted as vectors in which alignment can be readily quantified using basic trigonometric techniques. The cosine relationship of the angle between the EF and displacement vectors gives us a quantifiable alignment score between -1 and +1, where +1 is complete alignment of cell path to EF, and -1 is complete opposite alignment. Effect of Electric Field Magnitude on Vascular Cell Migration.

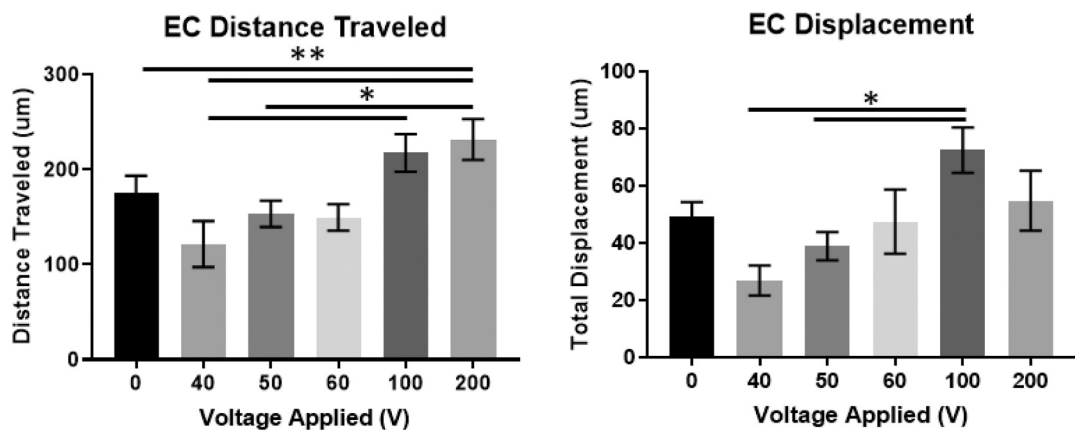
creating an EF that polarizes nearby cells and leads to their directional migration [43–45]. The response of cells to exogenous EFs has been found to vary widely in terms of direction and extent of their growth. In vascular cells specifically, prior research has identified vascular endothelial growth factor (VEGF) receptors as vital in their galvanotactic behavior [21,23]. Similarly, the responsiveness of cells and their galvanotactic behavior is further mediated by ion and growth factor concentrations in the surrounding media [46–48]. As it is known that VEGF and other factors are conducive to phenotypic switching of vascular cells, it would be relevant for future studies to investigate the phenotypic state of vascular cells under DCEF influence.

Furthermore, many vascular-focused studies have examined microvasculature ECs and smaller vessels for angiogenic applications. However, a previous study by Li et al. (2002) showed that ECs derived from bovine aorta migrated toward the cathode, while our studies and those of Bai et al. (2004) showed that ECs from smaller vessels migrated toward the anode [21,24]. Despite being of vascular endothelial origin, these cell types can behave very differently, suggesting a delicate relationship between their functionality from artery size and their galvanotactic response. For this reason, in this study we purposely chose human umbilical artery cells, being similar in size to coronary,

peripheral, and carotid arteries, which are often sites of atherosclerotic buildup or vascular intervention. In future studies, we plan to further simulate vascular diseased conditions by imposing an inflammatory and hypoxic environment on the cells to identify galvanotactic behavior under pathologic conditions. Previous research suggests that diseased, ischemic, or injured tissues become polarized, making them a good target for galvanotaxis [44,49].

Our previous studies and others have evidenced that migration is a dominating precursor to neo-intimal proliferation, for both ECs and SMCs during initial wound healing [50,51]. Although not specifically examined in this study, exogenous DCEF can influence cell proliferative behavior independent of their motility. Proliferation specifically is stimulated by higher magnitude, pulsing or alternating current EFs, compared to lower-magnitude direct current fields [38,44,49]. In an effort to elucidate migration modulation only, we explored low-magnitude DCEFs. While our results confirmed negligible cell proliferation during 4 h of growth, the increased SMC and EC motility raises questions about the actin dynamics and cell morphology that are typical of non-quiescent ECs and SMCs.

A Endothelial Cell Motility



B Smooth Muscle Cell Motility

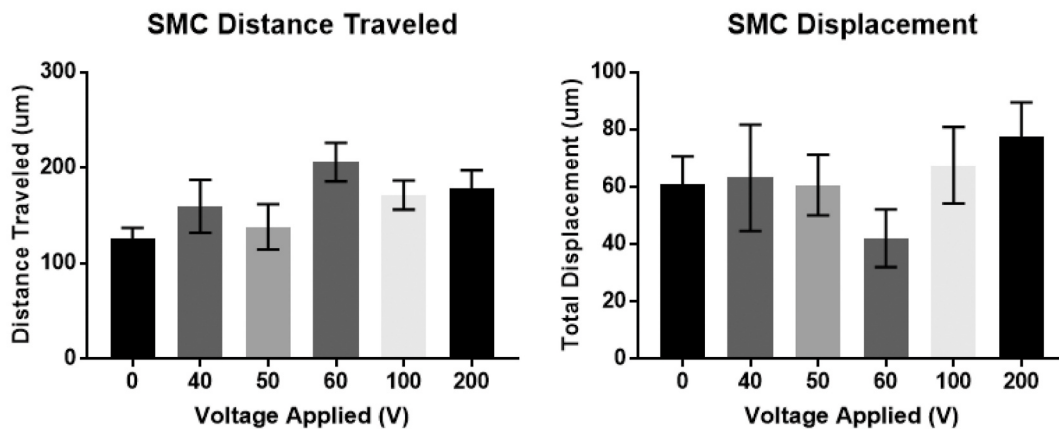


Fig. 5. Electric Field Magnitude and Vascular Cell Motility. (A) Distance of ECs traveled (left) and spatial displacement from their starting point (right) after 4 h of voltage applied to the galvanotaxis chamber. (B) SMCs distance (left) and spatial displacement traveled under the same conditions. Values are displayed as average of each cell path \pm standard error. Cell paths were quantified $n \geq 12$ times. ** denotes $p < 0.01$; * denotes $p < 0.05$.

A EC and SMC Migration Track Alignment to Electric Field

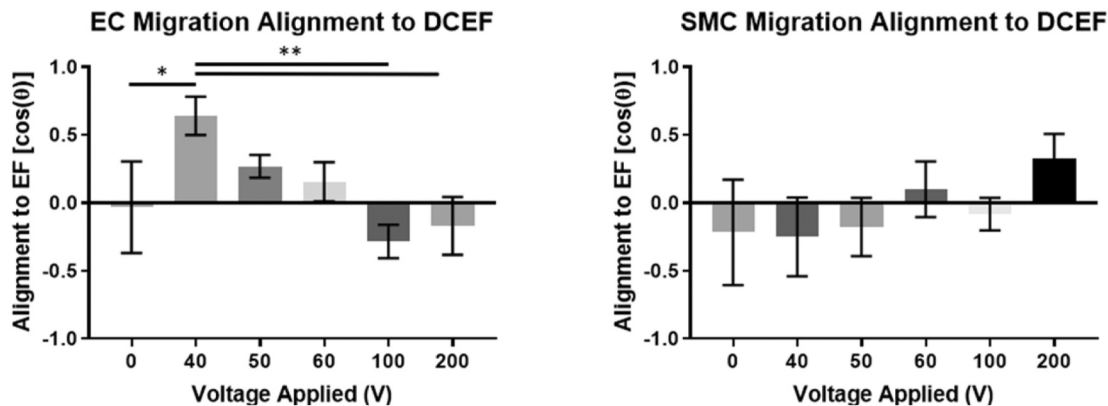
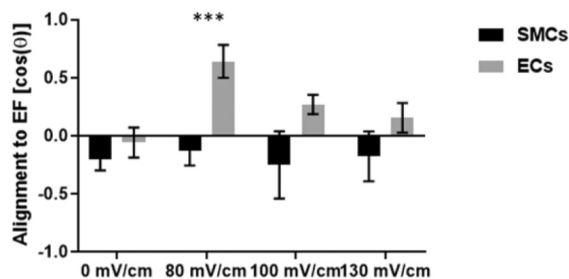


Fig. 6. Electric Field Magnitude and Vascular Cell Migration Direction. (A) EC location after migrating 4 h in galvanotaxis was quantified as it aligns to direction of DCEF, with increasing magnitude. (B) SMC alignment was similarly quantified. Alignment was quantified so that +1 denotes complete alignment towards direction of DCEF, -1 denotes complete opposite direction of migration in relation to EF. Values are displayed as average of each cell path \pm standard error. Cell paths were quantified $n \geq 12$ times. ** denotes $p < 0.01$. Comparison of EC and SMC Response to Electric Field.

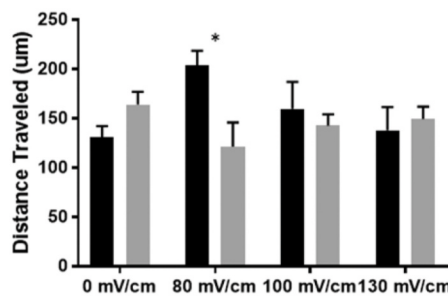
A Cell Migration Track Alignment by Electric Potential

SMC vs EC Alignment to Electric Field



B

SMC vs EC Distance Traveled



C

SMC vs EC Displacement

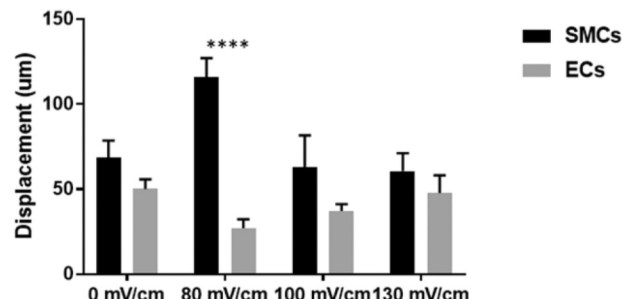


Fig. 7. Differential Vascular Cell Behavior and Measured Electric Potential. (A) SMC and EC cell direction in relation to the DCEF direction, normalized to the electric potential felt by cells in their respective media. From highest difference in migration direction with electric potential, (B) vascular cell migration distance (C) and displacement from origin. Values are displayed as average of each cell path \pm standard error. Cell paths were quantified $n \geq 12$ times. ** denotes $p < 0.01$.

4. Conclusions

Application of DCEFs to vascular endothelial and smooth muscle cells notably influences their migration. This influence impacts both migratory direction and extent of migration. Compared to migration distance and displacement, directionality is more evidently dominant in the differential galvanotactic response between vascular ECs and SMCs. This behavior offers potential for a desired clinical therapeutic if advanced in translation, as a means of preferentially advancing endothelial cell vascular surface coverage, while coordinately retarding smooth muscle cell ingrowth. As such, in considering the translation of galvanotaxis to an implant (stent) or catheter therapeutic, incorporation of electrodes, their device-specific geometry and design will be critical and must be carefully considered to preserve this differential migratory behavior. With further investigation galvanotaxis as an “electroceutical” may have potential for more generally improving cell-specific wound healing in the vasculature.

5. Methods

5.1. Galvanotaxis System Overview

All experiments were performed within a custom-designed microscope chamber (OKO Labs) for a Zeiss Axiovert 135, and regulated at 37 °C and 5% CO₂ (Fig. 1A). A sterile water reservoir was included in the chamber, to maintain high relative humidity. The galvanotaxis platform was held in place with a microscope stage with 60-mm dish housing. Cells in the galvanotaxis chamber were visualized through a 10X objective lens. External to the microscope chamber, a DC power supply (BK Precision 9184B) was attached via cable clips to the galvanotaxis powering Ag/AgCl electrodes. The microscope was also attached to an

external computer-controlled Retiga R3 microscope camera (QImaging) for imaging at 5- minute intervals, using Micro-Manager (μ Manager) and ImageJ (NIH) software.

5.2. Galvanotaxis platform fabrication

The galvanotaxis chamber was designed with SolidWorks software and 3-D printed with ABS plastic (QIDI Tech I; Fig. 2). Before use in experiments, chambers were submerged in DI water overnight, rinsed with 70% (v/v) ethanol, followed by a final rinse with DI water. Electrically insulating silicon grease (DC4, Dow Corning) was carefully applied to the bottom of the chamber around each well, the chamber was then sealed to the bottom of a 60-mm tissue culture-treated polystyrene dish (NUNC Thermo Scientific). Excess grease was cleaned out with a sterile pipette tip and the chamber was rinsed with distilled water then allowed to air dry overnight. Chambers in dishes were UV treated for 15 min on each side before use with cells.

5.3. Ag/AgCl electrode fabrication

Ag/AgCl electrodes used to power the galvanotaxis experiments were created by cutting 6 cm of Ag wire (Alfa Aesar; 1.0 mm diameter) and incubating 2 cm of the ends in bleach (6% sodium hypochlorite; Clorox) for 15 min at room temperature. The AgCl portion of the wire was then submerged in distilled water for 5 min followed by air drying. Ag/AgCl electrodes were bent at 90° angle and AgCl end was placed in the electrode holder in the saline chamber of the galvanotaxis platform.

5.4. Agar salt bridge fabrication

To create an ionically conductive bridge, agar was formed by

